^{6}Li and ^{7}Li induced fission of ^{232}Th and ^{238}U†

H. Freiesleben,* G. T. Rizzo,‡ and J. R. Huizenga
Nuclear Structure Research Laboratory§ and Departments of Chemistry and Physics, University of Rochester, Rochester, New York 14627
(Received 30 December 1974)

The energy dependence of the total fission cross section, the fragment angular distribution, and the fragment correlation angle were measured for ^{6}Li and ^{7}Li induced fission of ^{232}Th and ^{238}U at bombarding energies of 24–38.4 MeV. Angular distributions of elastically scattered projectiles for the four systems were measured at 37.2 MeV. Characteristic differences were found for ^{6}Li and ^{7}Li projectiles which are independent of the target. These differences include (1) the ^{7}Li induced fission has a larger anisotropy, (2) the energy dependence of the fragment anisotropy shows more structure for ^{7}Li, and (3) at low bombarding energy the cross section for ^{6}Li induced fission is considerably larger. These factors are discussed in terms of (1) competition between compound nucleus fission and fission following transfer reactions and (2) the deexcitation branching ratios between neutron emission and fission.

[NUCLEAR REACTIONS ^{232}Th(^{6,7}Li, f), ^{238}U(^{6,7}Li, f) E = 24–38.4 MeV, measured $W(165°)/W(90°)$, $\sigma_f(\theta)$, $\sigma_{el}(\theta)$ at 37.2 MeV, $\sigma_f(E)$.]

I. INTRODUCTION

Fission of heavy elements has been studied with a large number of light and heavy projectiles over a wide range of energies.[1] Although lithium induced fission of bismuth has been investigated recently,[2] no information is available on very heavy fissionable targets. Hence, the present experiments were undertaken to study ^{6}Li and ^{7}Li induced fission of ^{232}Th and ^{238}U. The energy dependence of the total fission cross section, the fragment anisotropy, and the fragment correlation angle were studied as well as the elastic scattering of ^{6}Li and ^{7}Li for projectile energies ranging from 24 to 38.4 MeV. Insofar that the transfer cross sections of lithium-ion induced reactions near and below the Coulomb barrier are relatively large,[3] such reactions have the possibility of transferring more than full linear momentum to the composite nucleus. This property of lithium-ion induced reactions is of great interest in lifetime experiments, especially for fission isomers.

II. EXPERIMENTAL METHODS AND RESULTS

The Emperor Van de Graaff facility of the Nuclear Structure Research Laboratory has been used to provide ^{6}Li and ^{7}Li beams. Beam energies between 24 and 38.4 MeV have been used. Targets of ^{232}Th and ^{238}U were prepared by evaporating natural ThF_4 and UF_4 onto 40-μg/cm^2 carbon backing foils. The thicknesses of Th and U were determined by Rutherford scattering of ^{6}Li ions to be (83 ± 3) and (118 ± 4) μg/cm^2, respectively. The targets were carefully centered in a multipurpose scattering chamber and solid state detectors were used to detect the scattered Li ions and the fission fragments.

A. Scattering of ^{6}Li and ^{7}Li from ^{232}Th and ^{238}U

Angular distributions of scattered projectiles were taken at 37.2-MeV incident beam energy using five surface barrier detectors simultaneously. The detectors were mounted with a fixed angular distance of 15° and moved together between 30° and 170°. An additional detector served as a monitor. Less detailed data were taken at 24 and 32 MeV. The resolution of the detectors was not good enough to discriminate particles inelastically scattered to the excited 2^+ and 4^+ states of the targets. In order to see whether the inelastic processes are due to nuclear scattering or Coulomb excitation, high resolution spectra of inelastically scattered ^{6,7}Li ions from ^{232}Th and ^{238}U were taken at 140° with an Enge spectrograph at a bombarding energy of 32 MeV.

The cross sections for elastic and inelastic scattering were compared with the predictions of a Coulomb excitation code,[4] where the reduced transition matrix elements were taken from the literature.[5] Very good agreement was found. Hence, we conclude that the inelastic scattering is mainly due to Coulomb excitation, and contribu-

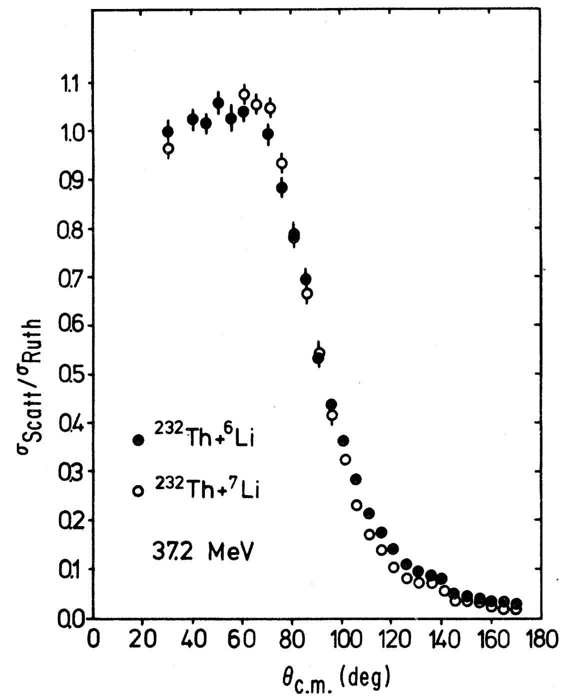

FIG. 1. Angular distributions of scattered ^{6}Li and ^{7}Li particles from ^{232}Th at 37.2-MeV bombarding energy. The statistical errors of the data are smaller than the dot size.

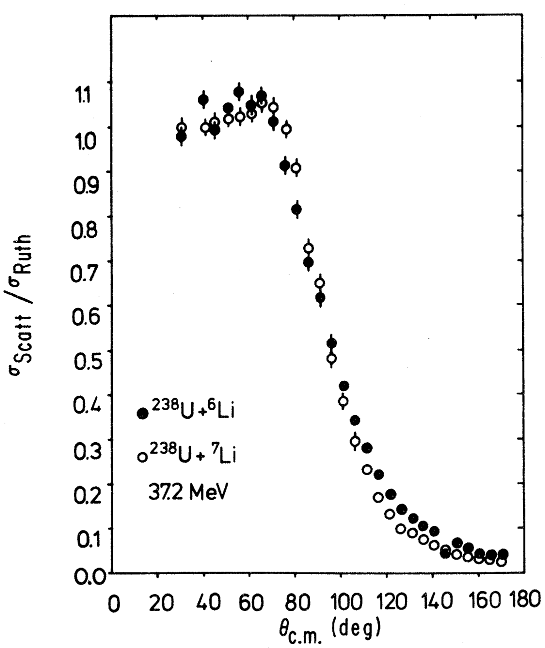

FIG. 2. Angular distributions of scattered ^{6}Li and ^{7}Li particles from ^{238}U at 37.2-MeV bombarding energy. The statistical errors of the data are smaller than the dot size.

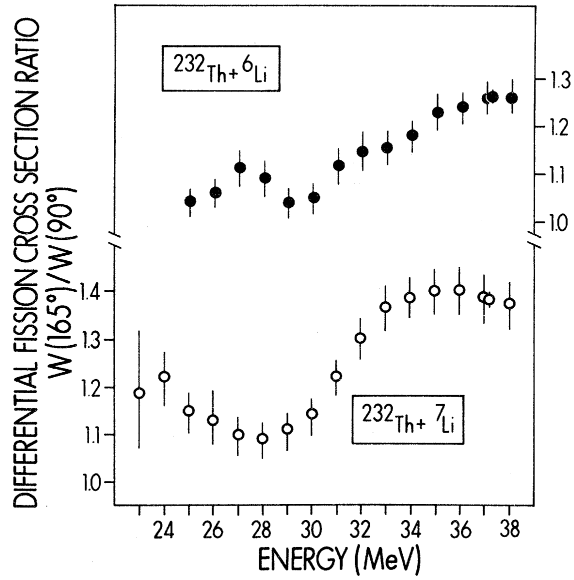

FIG. 3. Differential fission cross section ratios, $W(165°)/W(90°)$, for ^{6}Li and ^{7}Li induced fission of ^{232}Th as a function of bombarding energy.

tions from inelastic nuclear scattering are negligible at least at this energy. Consequently the unresolved groups of inelastically scattered projectiles were treated as part of the elastic group in the analysis and theoretical interpretation.

The differential scattering cross section results are displayed in Figs. 1 and 2. We point out two general features: (1) Since the data were taken

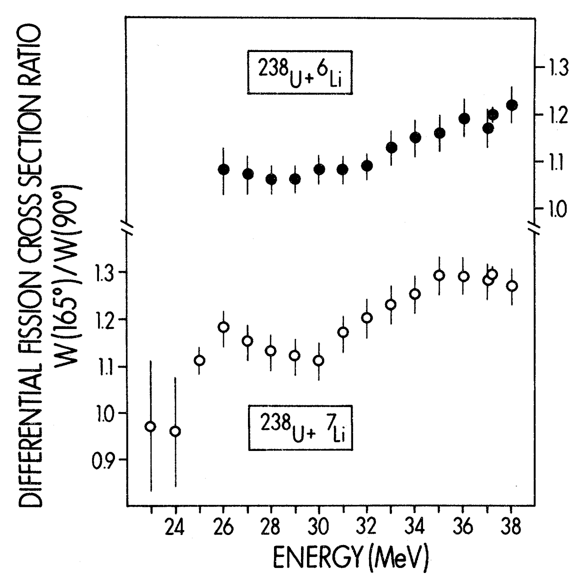

FIG. 4. Differential fission cross section ratios, $W(165°)/W(90°)$, for ^{6}Li and ^{7}Li induced fission of ^{238}U as a function of bombarding energy.

at energies only a few MeV above the Coulomb barrier, the angular distributions are rather smooth and do not reveal a prominent structure. At scattering angles close to the grazing angle the measured scattering cross sections are slightly larger than the Rutherford cross sections. This enhancement is due to interference between the nuclear and Coulomb scattering amplitudes.

(2) For both targets the ^{6}Li and ^{7}Li scattering is characterized by a small but significantly different angular dependence. The ^{7}Li projectiles give a more rapid decrease in cross section with scattering angle.

B. Fission fragment anisotropy

The differential fission cross section ratios, $W(165°)/W(90°)$, for ^{6}Li and ^{7}Li induced fission of ^{232}Th and ^{238}U were measured between 23 and 38 MeV. The angle between the two surface barrier detectors, located at 90° and 165° and having the same geometry, was bisected by the plane of the target foil. Hence, small changes in the beam position made a negligible change in the cross section ratio.

The energy dependence of the ratio $W(165°)/W(90°)$ in the center-of-mass (c.m.) system is shown for each of the above four reactions in Figs. 3 and 4. In addition, more detailed angular distributions have been measured at 37.2 MeV for these reactions using five detectors simultaneously. These results are shown in Figs. 5 and 6 and include a least squares fit of Legendre polynomials to the data, using the equation

$$W(\theta_{\rm cm}) = W(90°) \sum_{L=0}^{L_{\max}} a_{2L} P_{2L}(\cos\theta_{\rm cm}) \,. \qquad (1)$$

The coefficients obtained by fitting the experimental data are listed in Table I. Inclusion of a term with $L=3$ did not improve the fit and indicates that only angular momenta $L \leqslant 2$ between the two fragments are relevant.

From a comparison of the data for the same target in Figs. 3 and 5 and in Figs. 4 and 6, one observes that the ^{7}Li induced fission shows a larger anisotropy. This is expected from the fact that Γ_n/Γ_f is larger for the initial compound

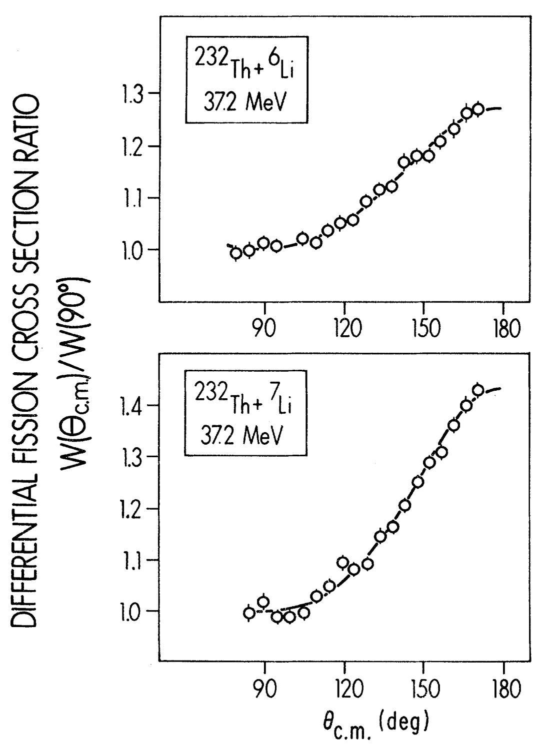

FIG. 5. Differential fission cross section ratios, $W(\theta_{\rm c.m.})/W(90°)$, for ^{6}Li and ^{7}Li induced fission of ^{232}Th at 37.2-MeV bombarding energy as a function of the center-of-mass angle $\theta_{\rm c.m.}$.

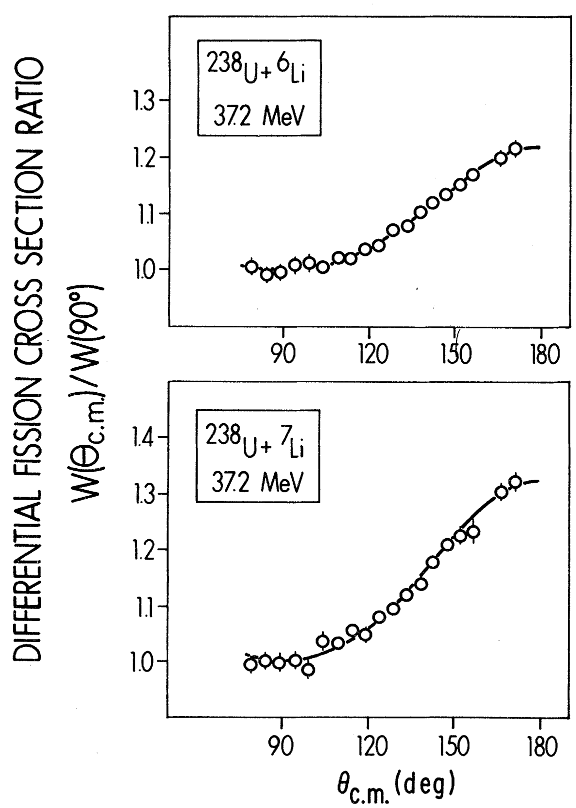

FIG. 6. Differential fission cross section ratios, $W(\theta_{\rm c.m.})/W(90°)$, for ^{6}Li and ^{7}Li induced fission of ^{238}U at 37.2-MeV bombarding energy as a function of the center-of-mass angle $\theta_{\rm c.m.}$.

TABLE I. Legendre coefficients obtained from a least squares fit to the fission fragment angular distributions at 37.2 MeV incident energy.

Reaction	a_0	a_2	a_4
^{232}Th + ^{6}Li	1.079 ± 0.032	0.173 ± 0.049	0.020 ± 0.007
^{232}Th + ^{7}Li	1.107 ± 0.030	0.259 ± 0.054	0.059 ± 0.010
^{238}U + ^{6}Li	1.060 ± 0.013	0.136 ± 0.024	0.020 ± 0.005
^{238}U + ^{7}Li	1.091 ± 0.024	0.204 ± 0.042	0.030 ± 0.008

nucleus with one more neutron. Since the anisotropy for a fixed angular momentum distribution increases with decreasing excitation energy, more later-chance fission (at lower excitation energy in the respective nuclei) increases the anisotropy. The same effect is reflected in the sudden increase of the anisotropy of ^{7}Li induced fission when a new (^{7}Li, xnf) channel opens. This occurs at ^{7}Li energies of about 24 MeV (^{7}Li, $3nf$) and 31 MeV (^{7}Li, $4nf$) as can be seen in Figs. 3 and 4. The threshold effect is less obvious in ^{6}Li induced fission on both targets. This is one of the unexpected characteristic differences between ^{6}Li and ^{7}Li induced fission.

C. Total fission cross section

The total fission cross section is obtained by integrating the differential fission cross section. For the lithium-ion energy of 37.2 MeV, we have compared the total fission cross section obtained using the coefficients from the Legendre polynomial fit (Table I) and coefficients where only relative angular momenta $L = 0$ and $L = 1$ are assumed between the fission fragments. The results are equal within the statistical errors of our data. Hence, the anisotropy ratio $W(165°)/W(90°)$ was used to determine the ratio a_2/a_0. Since $W(90°)$ was obtained absolutely in the anisotropy measurements, the total fission cross section was calculated at each energy from these experimental data.

At low beam energies, pileup from elastic scattering may mask the fission events. In order to check the data in an independent experiment, measurements of correlated fragments have been performed. A surface barrier detector placed at 90° was collimated to subtend an angle of ±1° at the target, while a second detector, subtending an angle of ±12°, was mounted so that complementary fragments of all fission fragments in the first detector were incident on the second one. For the second detector, the appropriate correlation angle as determined for 30-MeV lithium ions (see Sec. II D) was used. The large solid angle assures that each pair of fission fragments was de-

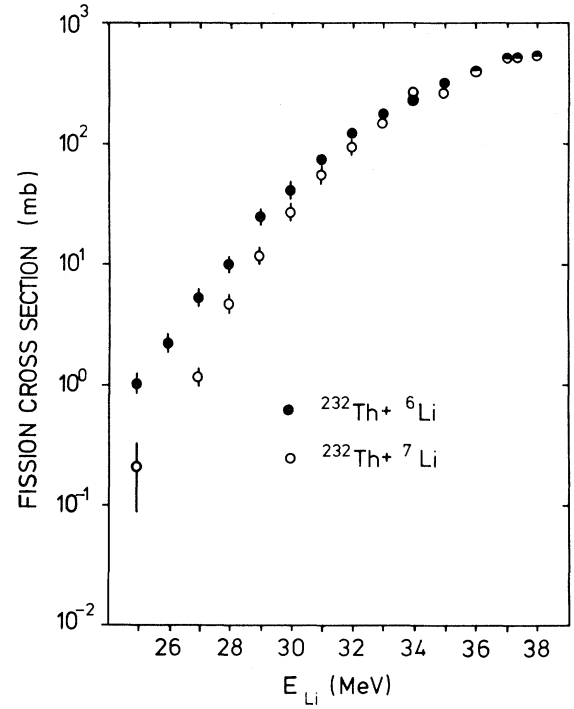

FIG. 7. Total fission cross sections for ^{6}Li and ^{7}Li induced fission of ^{232}Th as a function of the bombarding energy. The statistical error is smaller than the data point size when no error bar is shown.

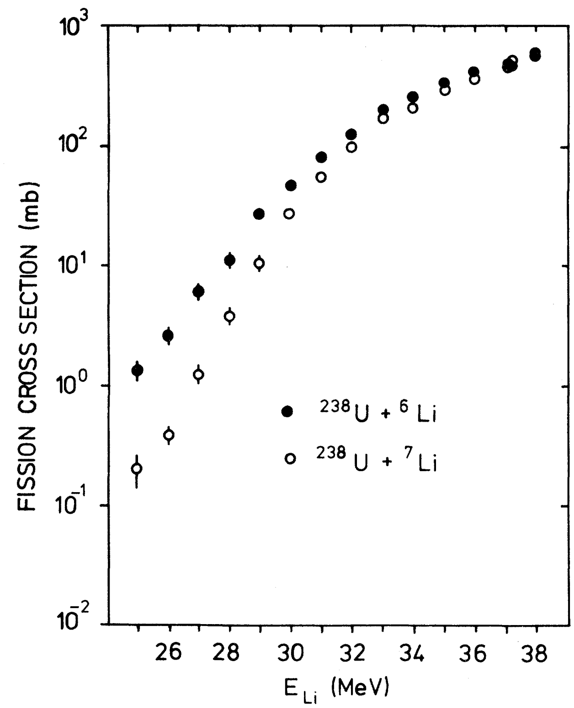

FIG. 8. Total fission cross section for ^{6}Li and ^{7}Li induced fission of ^{238}U as a function of the bombarding energy. The statistical error is smaller than the data point size when no error bar is shown.

TABLE II. Experimental fission cross sections as a function of bombarding energy.

E_{lab} (MeV)	$^{232}Th+^{6}Li$ σ (mb)	$^{232}Th+^{7}Li$ σ (mb)	$^{238}U+^{6}Li$ σ (mb)	$^{238}U+^{7}Li$ σ (mb)
25	1.0± 0.2	0.21± 0.13	1.4± 0.3	0.20± 0.05
26	2.2± 0.4		2.6± 0.4	0.39± 0.06
27	5.2± 0.6	1.2 ± 0.2	6.0± 0.6	1.3 ± 0.1
28	9.8± 2.0	4.7 ± 0.5	11.3± 1.2	3.9 ± 0.3
29	25.0± 1.8	11.8 ± 1.1	27.5± 1.9	10.6 ± 0.6
30	41 ± 6	26.8 ± 2.1	47 ± 7	27.5 ± 1.4
31	72 ± 11	57 ± 4	83 ± 6	53 ± 2
32	123 ± 7	103 ± 4	127 ± 6	96 ± 2
33	176 ± 26	166 ± 25	204 ± 9	177 ± 4
34	249 ± 25	269 ± 27	258 ± 26	240 ± 10
35	327 ± 33	298 ± 30	329 ± 33	307 ± 31
36	401 ± 40	411 ± 41	413 ± 41	368 ± 37
37	511 ± 51	536 ± 54	468 ± 47	436 ± 44
37.2	523 ± 26	537 ± 27	488 ± 25	525 ± 27
38	564 ± 56	564 ± 56	525 ± 53	524 ± 53

tected at all beam energies. The results from the single fragment spectra at 90° were in very good agreement with the results from the coincidence measurements requiring correlated fragments.

The experimental total fission cross sections for $^{232}Th+^{6,7}Li$ and $^{238}U+^{6,7}Li$ are displayed in Figs. 7 and 8. The curves in these figures have the well known shape of fission excitation functions at incident energies near the Coulomb barrier (≈33 MeV). At such energies barrier penetration has a dominant effect on the compound nucleus formation cross section and, hence, the fission cross section. A remarkable difference between the ^{6}Li and ^{7}Li induced fission cross section is found. The ($^{6}Li,f$) cross section is roughly five times larger than the ($^{7}Li,f$) cross section at the lowest energy. The difference in cross section disappears at higher bombarding energies. The numerical results for the total fission cross sections of each of the four systems which were studied are given in Table II.

D. Fragment correlation angle measurements

The fragments of a binary fission process are emitted in opposite directions in the center-of-mass system. Due to the center-of-mass motion, the correlation angle measured in the laboratory system is less than 180°. For a special geometry where one fragment is detected at $\theta_2=-90°$ in the laboratory, the most probable correlation angle for the other fragment follows from two-body kinematics

$$\sin^2\theta_{mp}(1)=(1-x_1^2)/(1+2x_1x_2+x_2^2)\ , \tag{2}$$

where $x_i^2=M_{fi}M_P E_P/E_{fi}M_{cn}^2$, $\theta_{mp}(1)$ is the most probable laboratory angle of fragment 1, M_P and E_P are the projectile mass and laboratory energy, and M_{fi} and E_{fi} are the mass and the c.m. energy of fission fragment i. Experimental measurements of the above angle give a distribution of values centered around θ_{mp}. This is due to asymmetric mass division and neutron emission prior to or after fission which is not taken into account in Eq. (2). Since θ_{mp} depends on the momentum transferred by the projectile to the target, the correlation angle measurement has often been used at energies above the Coulomb barrier to distinguish between fission following compound nucleus formation [referred to as full-momentum transfer (FMT)] and fission following direct interactions [referred to as incomplete momentum transfer[6] (IMT)]. Events due to IMT lead to correlation angles which are larger than those of FMT events. This produces an asymmetry in the correlation function on the large angle side.

We applied this method to $^{6,7}Li$ induced fission of ^{232}Th and ^{238}U in order to investigate the percentage of the fission cross section which is due to FMT. Measurements were performed at Li ion energies of 30 and 38.4 MeV. Fission fragments were detected with surface barrier detectors. In order to have a large solid angle without losing angular resolution, rectangular apertures of 2×15 mm^2 were used, subtending ±0.8° in the reaction plane and ±6.1° perpendicular to the reaction plane. The angular position of the detectors was checked by means of a telescope and found to be accurate to 0.1° with respect to the beam axis, which was defined by three aligned apertures. Standard electronics, including a time-to-pulse-height converter, were used to de-

TABLE III. Comparison of measured and calculated [Eq. (2)] correlation angles.

Projectile	E (MeV)	^{232}Th Target θ_{meas}	FWHM	θ_{calc}	^{238}U Target θ_{meas}	FWHM	θ_{calc}
^{6}Li	30.0	80.6± 0.1	5.9± 0.1	82.3			
^{6}Li	38.4	79.2± 0.1	5.2± 0.1	81.4	80.2± 0.1	4.8± 0.2	81.6
^{7}Li	38.4	78.8± 0.1	5.0± 0.1	80.7	80.2± 0.1	4.8± 0.1	81.0

tect and to discriminate accidental and real coincident events. By moving one detector coincident counts were obtained as a function of angle. Special care was taken to establish the target position because large errors in the correlation angle can be introduced by a target displacement along the beam axis. The target position was checked by Li-Li scattering, making use of the fact that for elastic scattering of identical particles the angle between scattered and recoiled particles is 90°. The results obtained from a correlation experiment for the ^{232}Th + ^{6}Li reaction at an energy of 38.4 MeV are shown in Fig. 9. The solid line is a Gaussian distribution fitted to the experimental points. From the nearly symmetric shape

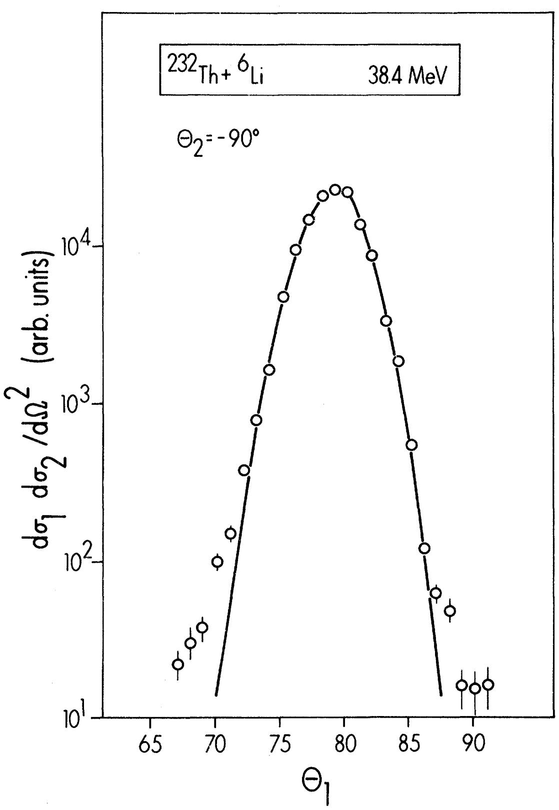

FIG. 9. Correlation angle between fission fragments from a ^{6}Li bombardment of ^{232}Th at 38.4 MeV. The solid line is a fitted Gaussian distribution.

of the data plotted in Fig. 9, we conclude that less than 4% of the fission cross section follows IMT at an energy of 38.4 MeV. A summary of the results for different energies and reactions is given in Table III.

III. DISCUSSION

The comparison of ^{6}Li and ^{7}Li induced fission provides a means to study the role of the additional neutron brought in by ^{7}Li. One expects that after evaporation of the first neutron, the fission process induced with ^{7}Li projectiles with energy E proceeds in analogy to that induced with ^{6}Li projectiles with energy $E-(E_B+\epsilon)$, where E_B is the neutron binding energy of the first emitted neutron and ϵ is its average kinetic energy. Differences, for example, in the angular distributions of fission fragments from ^{6}Li and ^{7}Li induced fission may be attributed to first-chance fission following ^{7}Li capture, that is, to the additional neutron.

In practice, this comparison turns out to be rather difficult. The angular momenta in the ^{7}Li entrance channel at energy E and in the ^{6}Li entrance channel at energy $E-(E_B+\epsilon)$ are quite different at energies in the vicinity of the barrier. Therefore, quite different K states (K is defined by the projection of the transition state spin on the nuclear symmetry axis) are contributing to the anisotropy of the fission fragments. Due to the similarity of Q values for compound nucleus formation with ^{6}Li and ^{7}Li, the excitation energies of the initial compound systems differ by approximately $E_B+\epsilon$. Since the variance K_0^2 is energy-dependent, the resulting K distributions given by $F(K)\propto \exp(-K^2/2K_0^2)$ are different.

In a second- or later-chance fission process, the emitted neutrons produce residual nuclei with a spin distribution which is slightly different from that of the original compound nucleus. In particular, the initial spin alignment (projection of the angular momentum on the space fixed axis; the projection M is zero if the target and projectile spin are each zero) is altered after neutron emission. Furthermore, for reactions where the anisotropy is small, it is necessary to include the projectile and target spins in calculations of the fragment anisotropy for particle induced fission.[7]

For reactions induced with projectiles of low energy, the above-mentioned factors may be significant since the spins of the initial compound nuclei are not necessarily large compared with the angular momentum carried away by evaporated neutrons. Hence, in a three- or four-chance fission process, it is very difficult to interpret the measured angular distributions in terms of reliable K_0^2 distributions of the initial and intermediate compound nuclei.

The above argumentation is based on the assumption that fission occurs after the amalgamation of the projectile and target. However, this is not the only relevant process which can lead to fission. From a study of the ^{209}Bi + ^{7}Li reaction it is known[2,3] that for Li projectiles at energies near and below the Coulomb barrier, the compound nucleus cross section is smaller than the cross section for transfer reactions, while at higher bombarding energies the transfer cross section becomes negligible relative to the compound nucleus cross section. Transfer means in this connection any process where nucleons are exchanged between the projectile and the target without specifying the reaction mechanism. It can be a direct process or a Coulomb breakup of the projectile followed by absorption of either projectile fragment. This kind of a reaction produces, in the case of a ^{209}Bi target, residual nuclei which cannot undergo fission since their fission barriers are higher than the excitation energies involved.

With very heavy targets it is possible to produce fissionable nuclei following a transfer reaction of the type ^{238}U(^{7}Li, α)^{241}Np. Therefore, in the vicinity of the barrier the fission cross section is a sum of the cross sections from compound nucleus fission and fission following transfer reactions. The relative magnitude of the two types of fission is generally unknown, although differences in the transfer cross sections with ^{6}Li and ^{7}Li projectiles have been measured. After bombardment of ^{232}Th targets with ^{6}Li and ^{7}Li ions of 26.5 to 37.5 MeV, Fleury[8] has found activities due to ^{232,233}Pa. We assume, in analogy to the ^{209}Bi + ^{7}Li reaction,[3] that these activities are due to the (Li, αnx) transfer reactions. For a ^{209}Bi target,[3] the ^{6}Li transfer reaction systematically has a larger cross section than the ^{7}Li transfer reaction; however, this difference decreases at higher bombarding energies. These experimental results are probably due to the weak binding of ^{6}Li compared with ^{7}Li, a factor which favors transfer from or breakup of the ^{6}Li ions. If one takes into account the neutron-to-fission width ratios which are of the order of 2 for these Pa isotopes,[9] one verifies that fission following transfer reactions is important for low Li bombarding energies, especially for ^{6}Li projectiles.

The differences in the ^{6}Li and ^{7}Li induced fission cross sections at low bombarding energies are best explained as due to the different magnitudes of the contributions of ^{6,7}Li transfer reactions followed by fission. Thus, the fission with ^{7}Li ions is more likely to proceed via a compound nucleus than that with ^{6}Li ions. As a consequence, the anisotropy of ^{7}Li fission shows more structure with energy. In the case of ^{6}Li the structure is smeared out to a larger extent by fission following transfer reactions. We assume that the same mechanism is responsible for the differences in the fission of ^{238}U with Li ions as for ^{232}Th, although the data of Fleury are limited to the ^{238}U + ^{7}Li system at bombarding energies above 32.5 MeV. These data show that the (^{7}Li, $3n$) cross section is small compared with the fission

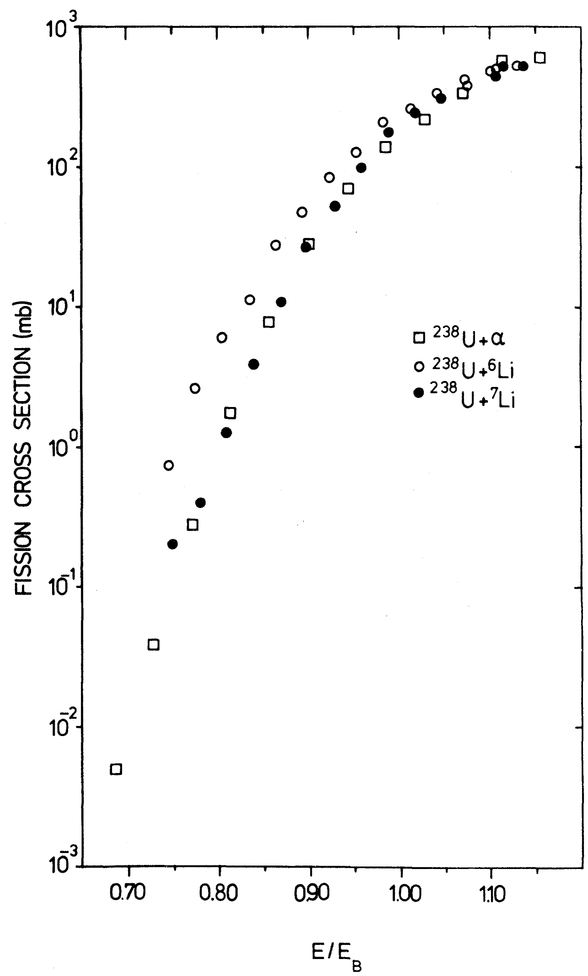

FIG. 10. Total fission cross sections for α, ^{6}Li, and ^{7}Li induced fission of ^{238}U as a function of the ratio of projectile energy to barrier height for each respective system.

cross section. The only other reported activity is due to ^{238}Np, presumably from the (^{7}Li, $\alpha 3n$) reaction.

Our assumption that the ^{7}Li induced fission proceeds mainly via a compound nucleus mechanism is supported by a comparison of this data with data for α induced fission[10] of ^{233}U. In Fig. 10 a comparison of these total fission cross sections is given. The cross section is plotted versus the ratio of the projectile energy to the barrier height of the system under question [$E_B(^{238}\mathrm{U}+\alpha)=23.4$ MeV, $E_B(^{238}\mathrm{U}+{}^6\mathrm{Li})=33.6$ MeV, $E_B(^{238}\mathrm{U}+{}^7\mathrm{Li})=33.4$ MeV, lab system]. The (^{7}Li, f) and (α, f) excitation functions show a very similar energy dependence which is different from that for the (^{6}Li, f) reaction.

The interpretation that fission following transfer reaction competes with compound nucleus fission is consistent with the correlation angle measurements (Sec. II D). A symmetric correlation angle distribution at low incident energies does not necessarily prove that a compound nucleus has been formed. Sub-Coulomb transfer reactions give outgoing α particles which are peaked at backward angles.[11] In this case the fissioning system gets more than full-momentum transfer. The inclusion of these events can result in a broadening of the distribution and in a shift of the centroid to smaller correlation angles. The magnitude of the above effects depends on the angular distribution of the outgoing particles in the transfer process. The most probable correlation angles, calculated for full-momentum transfer with Eq. (2), are listed in Table III for several reactions. These calculations were performed with an average fission fragment total kinetic energy derived from systematics[12] of experimental kinetic energies. In addition, an asymmetric mass split was assumed with a mass ratio $M_H/M_L = 1.3$. However, the correlation angle θ_{mp} is insensitive to the assumption about the mass ratio. As can be seen from Table III, our measured values of θ_{mp} are slightly smaller than the calculated values. Even though the deviations between experiment and calculation are small, they may indicate that more than the full momentum has been transferred to the fissioning system, especially when ^{6}Li is used as a projectile.

IV. CONCLUSIONS

Experimental data are presented for the first time on ^{6,7}Li induced fission of ^{232}Th and ^{238}U. Comparison of the data obtained for the fissioning systems formed in ^{6}Li and ^{7}Li bombardments shows characteristic differences between the two projectiles which are independent of the target. The larger anisotropy of fission fragments from ^{7}Li fission compared with ^{6}Li fission is explained by differences in the neutron-fission competition which favors later-chance fission for the system formed with ^{7}Li. The anisotropy ratio, $W(165^\circ)/W(90^\circ)$, as a function of the bombarding energy shows structure which again seems to be connected with neutron-fission competition in the ^{7}Li case. The same data for the ^{6}Li system do not reveal any prominent structure. Total fission cross sections for ^{6}Li at low bombarding energies are larger by a factor of 5 than those of ^{7}Li induced fission. We suggest that the later two effects are due to contributions to the fission cross section from transfer reactions followed by fission. There is experimental evidence that this process is significant for ^{6}Li projectiles, but less important for ^{7}Li projectiles. At high bombarding energies the compound nucleus fission cross section makes the main contribution to the total reaction cross section and the cross section for fission following transfer is small.

One of us, H. F., gratefully acknowledges support of Deutsches Bundesministerium für Forschung und Technologie.

---

†Work supported in part by the U. S. Atomic Energy Commission.

*Permanent address: Fachbereich Physik, Universität Marburg, Federal Republic of Germany.

‡Present address: 640 Clay Road, Rochester, New York 14623.

§Supported by a grant from the National Science Foundation.

[1]R. Vandenbosch and J. R. Huizenga, *Nuclear Fission* (Academic, New York, 1973).

[2]H. Freiesleben, H. C. Britt, and J. R. Huizenga, in *Proceedings of the Third International Symposium on the Physics and Chemistry of Fission, Rochester, 1973* (International Atomic Energy Agency, Vienna, 1974), Vol. 1, p. 447.

[3]H. Freiesleben, H. C. Britt, J. Birkelund, and J. R. Huizenga, Phys. Rev. C 10, 245 (1974).

[4]A. Winther and J. de Boer, *Coulomb Excitation* (Academic, New York, 1966), p. 303.

[5]Th. Elze and J. R. Huizenga, Nucl. Phys. A187, 545 (1972).

[6]W. J. Nicholson and I. Halpern, Phys. Rev. 116, 175 (1959); T. Sikkeland, E. L. Haines, and V. E. Viola, Jr., Phys. Rev. 125, 1350 (1962); V. E. Viola, Jr., M. M. Minor, A. E. Salwin, R. O. Bondelid, and R. B. Theus, Nucl. Phys. A174, 321 (1971).

[7]J. R. Huizenga, A. N. Behkami, and L. G. Moretto, Phys. Rev. 177, 1826 (1969).

[8]A. Fleury, Ph.D. thesis, Université de Bordeaux, 1969 (unpublished).

[9]R. Vandenbosch and J. R. Huizenga, in *Proceedings of the Second United Nations International Conference on the Peaceful Uses of Atomic Energy* (United Nations, Geneva, Switzerland, 1958), Vol. 15, p. 284.

[10]H. Freiesleben and J. R. Huizenga, Nucl. Phys. A224, 503 (1974).

[11]O. Häusser, A. B. McDonald, T. K. Alexander, A. J. Ferguson, and R. E. Warner, Phys. Lett. 38B, 75 (1972).

[12]V. E. Viola, Jr., Nucl. Data A1, 391 (1966).